

## Pulsar discovery prospect of FASTA

Mengyao Xue<sup>1</sup>, Weiwei Zhu<sup>1,2</sup>, Xiangping Wu<sup>1,2</sup>, Renxin Xu<sup>3</sup>, Hongguang Wang<sup>4,5</sup>

<sup>1</sup> National Astronomical Observatories, Chinese Academy of Sciences, Beijing 100101, China; [mengyaoxue@nao.cas.cn](mailto:mengyaoxue@nao.cas.cn)

<sup>2</sup> Institute for Frontiers in Astronomy and Astrophysics, Beijing Normal University, Beijing 102206, China

<sup>3</sup> School of Physics, Peking University, Beijing 100871, China

<sup>4</sup> Department of Astronomy, School of Physics and Materials Science, Guangzhou University, Guangzhou 510006, China

<sup>5</sup> Great Bay Center, National Astronomical Data Center, Guangzhou, Guangdong 510006, China

Received 2023 Feb 6th; accepted 2023 Jun 2nd

**Abstract** The Five-hundred-meter Aperture Spherical radio Telescope (FAST) has discovered more than 650 new pulsars, which account for 20% of our known Galactic pulsar population. In this paper, we estimate the prospect of a pulsar survey with a radio telescope array to be planned — the FAST Array (FASTA), consists of six “FAST-type” telescopes. Such a sensitive radio telescope array would be a powerful instrument in probing the pulsar population deep into our Galaxy as well as in nearby galaxies. We simulate the FASTA pulsar discovery prospects with different Galactic pulsar population models and instrumental parameter combinations. We find that FASTA could detect tens of thousands of canonical pulsars and well-over thousands of millisecond pulsars. We also estimate the potential yield if the FASTA is used to search for pulsars from the nearby spiral galaxy M31, and find that it would probably discover around a hundred new radio pulsars.

**Key words:** stars: neutron — stars: pulsars: general — telescopes

### 1 INTRODUCTION

Pulsars are rapidly rotating neutron stars. So far, astronomers have discovered more than 3300 radio pulsars<sup>1</sup> (Manchester et al. 2005). The studies of pulsars have led to a number of important progress in the frontiers of astrophysics and physics, including the theory of gravitation, the stellar evolution, the matter distribution of our Galaxy, and the equation of state for ultra-dense matter. The extraordinary impact and prominent scientific applications of pulsar research have made it one of the key science projects for nearly every new generation of advanced radio telescopes.

There are two main types of radio pulsars: canonical pulsars (CPs) and millisecond pulsars (MSPs). CPs are generally thought to be the remaining core after the supernovae explosion of progenitor massive star ( $\sim 10$  to  $30 M_{\odot}$ ). The radio emission of CPs are powered by the pulsar’s rotation energy. Therefore, as CPs keep emitting radio signals, they will gradually spin down when they become older. For example, one of the youngest pulsars, the Crab pulsar, has a spin period of  $\sim 33$  ms. Old CPs can have a spin period as long as tens of seconds (e.g. Tan et al. 2018; Caleb et al. 2022). MSPs (Backer et al. 1982) are old, rapidly rotating neutron stars that have been ‘spun up’ or ‘recycled’ through the accretion of matter

---

<sup>1</sup> ATNF Pulsar Database v1.68; [www.atnf.csiro.au/research/pulsar/psrcat](http://www.atnf.csiro.au/research/pulsar/psrcat)

from a companion star in a close binary system. Their typical spin period is in the range of about  $\sim 1$ -30 milliseconds.

Pulsar surveys and the resulting pulsar discoveries are crucial resources for us to build up our understanding of the Galactic pulsar population. For example, the Parkes Multi-beam Pulsar Survey (PMPS, Manchester et al. 2001), which has discovered  $\sim 800$  pulsars initially (Manchester et al. 2001; Morris et al. 2002; Kramer et al. 2003; Hobbs et al. 2004; Faulkner et al. 2004) and 1038 after many passes of searches (e.g. Eatough et al. 2013; Knispel et al. 2013; Bates et al. 2013), provides a large sample of pulsar detections with uniform instrument settings. Using this sample, astronomers established basic models of the Galactic pulsar population, including their spatial, period, and luminosity distributions (Lorimer et al. 2006; Faucher-Giguère & Kaspi 2006). Lorimer et al. (2006) suggest there are  $(3.0 \pm 0.1) \times 10^4$  canonical pulsars beaming toward the Earth with luminosities above  $0.1 \text{ mJy kpc}^2$ , while Faucher-Giguère & Kaspi (2006) predict there are  $(1.2 \pm 0.2) \times 10^5$  detectable canonical pulsars in the Galaxy. However, some following pulsar surveys using other instruments such as Arecibo PALFA (Cordes et al. 2006), Green Bank North Celestial Cap pulsar survey (GBNCC; Stovall et al. 2014), and FAST Galactic Plane Pulsar Snapshot survey (GPPS; Han et al. 2021) suggest that the population extrapolated from PMPS might be overestimated. A possible explanation is that PMPS concentrates on the Galactic Plane which has a high density of pulsars (Swiggum et al. 2014; McEwen et al. 2020; Han et al. 2021).

In the early 1990s, as one of the early concepts of the Square Kilometre Array (SKA), Chinese radio astronomers proposed to build  $\sim 30$  large spherical reflectors in Guizhou, southwest China, with a diameter of roughly 200 to 300 m each. This design was referred to as the Kilometer-square Area Radio Synthesis Telescope (KARST; Peng & Nan 1998; Nan et al. 2002). Although it was not selected as the final design for the SKA, it led to the birth of Five hundred meter Aperture Spherical Telescope (FAST; Nan 2006; Nan et al. 2011; Li et al. 2018), currently the most sensitive single-dish radio telescope. Since the commissioning operation of FAST, a number of notable science outcomes in pulsar studies have been carried out (e.g. Qian et al. 2020; Cameron et al. 2020; Han et al. 2021, etc.).

Today, the plan of building large spherical reflectors array has once again been put on the agenda after the successful delivery and operation of FAST. Chinese radio astronomers are considering to extend FAST with several similar spherical telescopes to form a telescope array — the FAST Array (FASTA). The initial phase of FASTA will consist of three spherical reflectors, each reflector will be similar to the existing one (we will refer to Phase-I FASTA as FASTA3 hereafter). The second phase of FASTA will add another three reflectors and bring the total number to six (similarly, we will refer to Phase-II FASTA as FASTA6 hereafter). FASTA will perform both coherent and incoherent observations of pulsars, providing a substantially higher gain than any current system, and would be able to discover a large number of potentially observable pulsars in the northern sky. In terms of sky coverage, FASTA and SKA will complement each other.

In this work, we estimated the prospect of pulsar discoveries for the FASTA in the sky area with galactic latitude  $|b| < 10^\circ$ . We considered both the case of FASTA3 and FASTA6, as well as data analysis using the incoherent summing or coherent beam-forming methods. Such a pulsar survey will help us understand the galactic pulsar population, especially at the low luminosity end. In section 2, we describe various pulsar population models and survey parameters used in the simulations. In section 3, we present the population synthesis results and FAST/FASTA detection prospect predicted by different models. In section 4, we summarise our conclusion and discuss future work.

## 2 METHOD

### 2.1 The Galactic pulsar population models

There are two general types of models for the Galactic pulsar population, ‘snapshot’ type of models and ‘evolutionary’ type of models. Within the two types of models, there are sub-group models which apply different population distribution parameters.

A typical ‘snapshot’ model was built up by [Lorimer et al. \(2006\)](#), hereafter L06. They used the result from the Parkes Multi-beam Pulsar Survey (PMPS; [Manchester et al. 2001](#)) to derive the optimal Galactic pulsar distribution in period ( $P$ ), luminosity ( $L$ ), Galactocentric radial distance ( $R$ ), and Galactic scale-height ( $z$ ). L06 treated these distributions independently, and assumed that all the canonical pulsars follow the same, fixed distribution regardless of their age. The ‘snapshot’ type of model is a kind of simplified model, since those distributions actually evolve with pulsar age. For example, younger pulsars, on average, are brighter and spin faster. They are also located closer to the galactic plane (associated with their progenitor stars) than older pulsars. Thus, pulsars in different age groups should have different distributions of period, luminosity, and scale height.

The L06 type of model can be regarded as a ‘snapshot’ of an evolving population. Despite the fact that ‘snapshot’ type of models rely on fewer assumptions and have fewer degrees of freedom, which makes them easier to evaluate, it is still worthwhile to develop models that take evolution into account. [Faucher-Giguère & Kaspi \(2006\)](#), hereafter FK06, presented a typical practice of constructing an ‘evolutionary’ type of model. For comparison, FK06 additionally provided an ‘unevolved’ luminosity distribution which is one of the distribution model we applied in this work. Apart from FK06, a lot of efforts have also been made toward optimizing and applying evolutionary models in pulsar population synthesis, e.g. [Contopoulos & Spitkovsky \(2006\)](#); [Ridley & Lorimer \(2010\)](#); [Bates et al. \(2014\)](#); [Rajwade et al. \(2017\)](#); [Huang & Wang \(2020\)](#).

### 2.1.1 Snapshot type of models

The ‘snapshot’ type of models often contains the following input parameters: (1) period distribution; (2) luminosity distribution; (3) radial density  $R$  distribution; (4) scale height  $z$ .

The most widely accepted period distribution for ‘snapshot’ type of canonical pulsar population models is the lognormal distribution with a mean of  $\langle \log_{10}(\frac{P}{\text{ms}}) \rangle = 2.7$  and a standard deviation  $\sigma[\log_{10}(\frac{P}{\text{ms}})] = 0.34$ , suggested by L06 based on modeling the PMPS result using PSRPOP<sup>2</sup>. In this work, we apply this L06 lognormal distribution for our ‘snapshot’ type simulation of the canonical pulsar population.

For the luminosity distribution of CPs, instead of using the simple power law distribution (with a low-frequency cut-off) suggested by L06, we adopt the FK06 luminosity distribution. FK06 suggested a lognormal luminosity distribution to avoid the hard cut-off. Based on modeling the PMPS result, the mean and standard deviation of FK06 luminosity distribution are  $\langle \log_{10} L \rangle = -1.1$ ,  $\sigma[\log_{10} L] = 0.9$ .

For the beaming fraction of CPs in ‘snapshot’ type of models, [Emmering & Chevalier \(1989\)](#) provided a simple approach:

$$f(\alpha, \rho) = 2 \left( \frac{1}{4\pi} \int_{\theta_l}^{\theta_u} 2\pi \sin \theta d\theta \right) = \cos \theta_l - \cos \theta_u, \quad (1)$$

where  $\alpha$  is the inclination angle,  $\rho$  is the beam radius,  $\theta_l = \max(0, \alpha - \rho)$  and  $\theta_u = \min(\pi/2, \alpha + \rho)$ . One empirical way to estimate the beam radius  $\rho$  provided by [Gould \(1994\)](#), is to treat  $\rho$  as a function of the pulsar rotating period,  $\rho(P) = 5.4^\circ (\frac{P}{\text{s}})^{-1/2}$ , while  $\alpha$  is a uniformly chosen random value between  $(0^\circ, 90^\circ)$ . We will further discuss the effects of different beaming fraction models in Section 2.2 where we describe the role of calibration surveys for our simulation.

For the radial density distribution of CPs, L06 suggested a gamma distribution (applying NE2001 electron density model):

$$f(R) = A \left( \frac{R}{R_\odot} \right)^B \exp \left( -C \left[ \frac{R - R_\odot}{R_\odot} \right] \right), \quad (2)$$

where  $A = 41$ ,  $B = 1.9$ , and  $C = 5.0$ . This relation implies that the pulsar density is zero at  $R = 0$ , which is inconsistent with our understanding of the galaxy structure. To avoid this discrepancy and

<sup>2</sup> A FORTRAN package to carry out Monte Carlo simulation of the Galactic pulsar population developed by [Lorimer et al. \(2006\)](#) <http://psrpop.sourceforge.net/>

obtain nonzero density at  $R = 0$ , Yusifov & Küçük (2004), hereafter YK04, included an additional parameter  $R_1$  and used a shifted Gamma function, replacing  $R$  and  $R_\odot$  in Eq. (2) by  $X = R + R_1$  and  $X_\odot = R_\odot + R_1$ . With this model, YK04 obtained the best-fit result with a parameter set of  $A = 37.6$ ,  $B = 1.64$ ,  $C = 4.01$  and  $R_1 = 0.55$  kpc. In this work, we compare FAST and FASTA simulated pulsar survey detection prospects using both L06 and YK04 radial distributions.

For the scale height ( $z$ ) distribution of CPs, L06 found an optimal scale height of 180 pc using NE2001 electron density model. This number is significantly lower than the expected value of 300–350 pc from independent studies of the local CPs population (e.g. Mdzinarishvili & Melikidze 2004). When applying the ‘smooth’ electron density distribution model (Lyne et al. 1985), the optimal scale height, 330 pc, is consistent with the observed local CPs population (Lorimer et al. 2006); this is the value we used in this work.

To describe the Galactic MSP population with the ‘snapshot’ type of models, the approaches are similar to the aforementioned CPs cases. Note that the modeled parameters for MSPs are limited by the relatively small sample size of the currently known MSP population. For the period distribution of MSPs, Lorimer et al. (2015), hereafter L15, suggested a lognormal distribution with a mean  $\langle \log_{10}(\frac{P}{\text{ms}}) \rangle = 0.65$  and a standard deviation  $\sigma[\log_{10}(\frac{P}{\text{ms}})] = 0.25$ . For the luminosity distribution of MSPs, following Smits et al. (2009), we adopt the same luminosity distribution of canonical pulsars. The beaming fraction of MSPs we used is  $f(\alpha, \rho) = \cos \theta_l - \cos \theta_u$ , where  $\theta_l = \max(0, \alpha - \rho)$  and  $\theta_u = \min(\pi/2, \alpha + \rho)$ . As suggested by Kramer et al. (1998), the beam radius,  $\rho$ , is a constant value for MSPs. Here we apply  $\rho = 31^\circ$  which corresponds to  $\rho(P) = 5.4^\circ (\frac{P}{\text{s}})^{-1/2}$ ,  $P = 30$  ms. We use 500 pc as the scale height for the Galactic MSP population as suggested by Smits et al. (2009). For  $R$  distribution, we apply both the L06 and the YK04 radial distribution, respectively.

The input model parameters we applied to model the Galactic CP and MSP populations using the ‘snapshot’ type of models are summarised in Table 1.

### 2.1.2 Evolutionary type of models

The ‘evolutionary’ type of models also use the following parameters to describe the Galactic pulsar population: (1) period distribution; (2) luminosity distribution; (3) radial density  $R$  distribution; (4) scale height  $z$ . The main difference between the evolutionary type of models and the ‘snapshot’ type of models is that for the evolutionary type of models, those pulsar parameters are all described as a function of the pulsar age. In this work, we apply 1 Gyr for the maximum age of the canonical pulsar population, and 5 Gyr for the maximum age of the MSP population based on the current distribution of observational pulsar characteristic age (Rajwade et al. 2017).

The period distribution for the evolutionary type of models is described by: (1) the initial (birth) spin period distribution; (2) the pulsar spin-down model; (3) the pulsar age. FK06 developed a typical ‘evolutionary’ model, and found the optimal initial period distribution for canonical pulsars follows a normal distribution with the mean  $\langle P_0 \rangle = 300$  ms. The observed pulsar rotating period at the present day can be evaluated using the initial period and the age of the pulsar. The spin-down model depends on the braking index  $n$  and the magnetic field strength  $B$ . In this work, we adopt the FK06 spin-down model and initial period distribution for canonical pulsars. We note that other ‘evolutionary’ type models may employ a different spin-down model and initial period distribution (e.g. Contopoulos & Spitkovsky 2006).

The luminosity distribution is also age-dependent. Since the radiated energy of pulsars is thought to be originated from the loss of rotational energy, the luminosity distribution can be modeled as a function of its period ( $P$ , in units of s), and its period derivative ( $\dot{P}$ , in units of  $10^{-15} \text{ s s}^{-1}$ ). It is commonly assumed to be a power-law:  $L = \gamma P^a \dot{P}^b$ , while the values of  $a$ ,  $b$ ,  $\gamma$  may vary among different models (e.g. Lyne et al. 1975; Vivekanand & Narayan 1981; Faucher-Giguère & Kaspi 2006; Rajwade et al. 2017). The original ‘evolutionary’ model, FK06, found the optimal value for  $a$ ,  $b$ , and  $\gamma$  are:  $a = -1.5$ ,  $b = 0.5$ , and  $\gamma = 0.18$  based on the PMPS pulsar sample. In this work, we follow the FK06 model. As a comparison, we also test the luminosity distribution derived from the fan-beam model (Wang et al. 2014; Huang & Wang 2020). The luminosity function of the fan-beam model not only depends on  $P$

and  $\dot{P}$ , but also the emission geometry in the term of  $L = \kappa \frac{W}{P} P^{q-4} \dot{P} \rho_{\text{peak}}^{2q-6}$ , where  $\frac{W}{P}$  is the duty cycle and  $\rho_{\text{peak}}$  is the radial distance between the magnetic pole and the emission direction accounting for the pulse peak in units of degree. Following [Huang & Wang \(2020\)](#), we adopt  $\kappa = 10^{2.75}$ ,  $\frac{W}{P} = 5\%$ ,  $q = 1.25$  in our simulation. Unlike the case of the conal beam, in the fan beam model, the impact angle between the line of sight (LOS) and the magnetic axis may extend to  $90^\circ$ , which means our LOS would sweep across at least one emission beam from either one pole or the other pole, so the beaming fraction is always 1. While the default evolutionary model applied an empirical beaming fraction given by [Tauris & Manchester \(1998\)](#),  $f(P) = 0.09(\log P - 1)^2 + 0.03$ , which is a function of the pulsar period.

The current position of each simulated pulsar in our Galaxy is determined by its initial birth position (following the  $z$  and  $R$  birth distribution), and its birth velocity. According to FK06, the initial birth  $z$  distribution follows an exponential function with a relatively small scale height of 50 pc. This is consistent with the distribution of supernovae where massive stars end their lives. While for the  $R$  distribution, FK06 applied the YK04 radial distribution as the birth radial distribution. In this work, we have tried the L06 and the YK04 radial distributions as the birth radial distribution. For the pulsar birth velocity distribution, we assume a Gaussian distribution centred on 0 km/s with a width of 265 km/s for the birth velocity for each of the  $x$ ,  $y$  and  $z$  directions following [Rajwade et al. \(2017\)](#). The pulsar position will then evolve from its initial position according to its velocity and age, according to the model of the Galaxy gravitational potential ([Carlberg & Innanen 1987](#); [Kuijken & Gilmore 1989](#)).

For evolutionary MSP population models, we adopted the L15 distribution for their initial birth period, which is a lognormal distribution with average  $\langle \ln(\frac{P}{\text{ms}}) \rangle = 1.5$  and a standard deviation  $\sigma[\ln(\frac{P}{\text{ms}})] = 0.58$ . We have tried two types of  $L$  distribution: (1) the FK06 fixed lognormal distribution with  $\langle \log_{10} L \rangle = -1.1$ ,  $\sigma[\log_{10} L] = 0.9$ ; (2) the FK06 evolved power-law distribution model,  $L = \gamma P^a \dot{P}^b$ , where  $a = -1.4$ ,  $b = 0.5$ , and  $\gamma = 0.009$  ([Rajwade et al. 2017](#)). The initial birth  $z$  distribution we adopted is the same as the evolutionary model for canonical pulsars (CPs), which is an exponential function with a scale height of 50 pc (FK06). For  $R$  distribution, similar with our CPs simulation, we have tested both the L06 and the YK04 radial distributions as the birth radial distribution. For the pulsar birth velocity distribution, following [Rajwade et al. \(2017\)](#), we assume a Gaussian distribution centred on 0 km/s with a width of 80 km/s for the birth velocity for each of the  $x$ ,  $y$  and  $z$  directions.

The input model parameters we applied to model the Galactic CP and MSP populations using the evolutionary type of models are summarised in [Table 2](#).

Table 1: The model parameters used in snapshot mode simulation of CPs and MSPs.

Parameter	CP	MSP
Spin period distribution	L06 lognormal	L15 lognormal
$\langle \log_{10}(\frac{P}{\text{ms}}) \rangle$	2.7	0.65
$\sigma[\log_{10}(\frac{P}{\text{ms}})]$	0.34	0.25
Luminosity distribution	FK06 lognormal	FK06 lognormal
$\langle \log_{10} L \rangle$	-1.1	-1.1
$\sigma[\log_{10} L]$	0.9	0.9
Galactic $z$ -scale height	330 pc	500 pc
Radial distribution Model A	L06	L06
Radial distribution Model B	YK04	YK04
Spectral index Distribution	Gaussian	Gaussian
$\langle a \rangle$	-1.4	-1.4
$\sigma_a$	0.9	0.9
Population scaling surveys	PMPS+SWIL+SWHL	PMPS+SWIL+SWHL
Detected pulsar number in scaling surveys	1214	48

Table 2: The model parameters used in evolutionary mode simulation of CPs and MSPs.

Parameter	CP	MSP
Initial spin period distribution	FK06 Gaussian	L15 lognormal
$\langle \frac{P}{\text{ms}} \rangle$	300	—
$\sigma[\frac{P}{\text{ms}}]$	150	—
$\langle \ln \frac{P}{\text{ms}} \rangle$	—	1.5
$\sigma[\ln(\frac{P}{\text{ms}})]$	—	0.58
Luminosity distribution model A	FK06 evolutionary $L = 0.18P^{-1.5}\dot{P}^{0.5}$	FK06 evolutionary $L = 0.009P^{-1.4}\dot{P}^{0.5}$
Luminosity distribution model B	Fan beam model	FK06 lognormal
Initial Galactic $z$ -scale height	50 pc	50 pc
Radial distribution Model A	L06	L06
Radial distribution Model B	YK04	YK04
1-D velocity dispersion	265 km s <sup>-1</sup>	80 km s <sup>-1</sup>
Maximum initial age	1 Gyr	5 Gyr
Spectral index Distribution	Gaussian	Gaussian
$\langle a \rangle$	-1.4	-1.4
$\sigma_a$	0.9	0.9
Pulsar spin-down model	FK06	FK06
Beam alignment model	orthogonal	orthogonal
Braking Index	3.0	3.0
Initial B-field distribution	Log-normal	Log-normal
$\langle \log_{10} B(\text{G}) \rangle$	12.65	8.0
std( $\log_{10} B(\text{G})$ )	0.55	0.55
Population scaling surveys	PMPS+SWIL+SWHL	PMPS+SWIL+SWHL
Detected pulsar number in scaling surveys	1214	48

## 2.2 FAST and FASTA pulsar survey simulations

In this work, we used `PsRPopPy` to perform the simulation. The simulation process of `PsRPopPy` contains two main steps: (1). generate synthetic pulsar populations of the Milky Way Galaxy; (2). perform simulated surveys on the synthetic pulsar population using corresponding survey parameters.

When `PsRPopPy` generates synthetic pulsar populations of the Milky Way Galaxy, the overall idea of how it controls the total number of the pulsar populations is reversed to how we think about this question intuitively. It does not first assume a total Galactic neutron star population with a beaming fraction to get the population of the pulsars that beaming to us, and then estimate how many pulsars we can detect. On the contrary, it uses the real numbers of discoveries from existing pulsar surveys and the corresponding survey parameters to calibrate the total number of the synthesized pulsar population. The calibration surveys need to have a good enough completeness. A commonly used calibration pulsar survey is the PMPS survey which discovered over a thousand pulsars in a uniform setup. For example, [Rajwade et al. \(2017\)](#) applied the same detection threshold and observing ranges of the PMPS to their synthesized pulsar population with a pulsar detection sample size of 1065. In this case, `PsRPopPy` keeps generating new simulated pulsars until the generated population contains exactly 1065 pulsars detectable by the same setup as PMPS. All the pulsars generated in this process, if they are beaming toward us, are stored as the whole synthetic pulsar population for further analysis, no matter whether they are detectable by PMPS or not. While the simulated pulsars which are not beaming toward us are all left. In such a way, the total population mostly depends on the calibration surveys, while the beaming fraction is not a key dominant factor that directly affects the simulated detection number of pulsars. It affects the simulation result in a relatively secondary way due to its relation with other characteristics of pulsars, namely the pulsar rotating period  $P$ . Since longer period pulsars have smaller beaming fraction, the effect is like shifting the period distribution toward the shorter  $P$  end.

PsRPopPy can adopt multiple calibration surveys together as a whole when generating synthetic pulsar population. Here, following Huang & Wang (2020), we adopt a combination of PMPS, together with two Swinburne pulsar surveys (SWIL, Edwards et al. 2001; and SWHL, Jacoby et al. 2007) as calibration surveys. This provides us a sample of 1214 canonical pulsars (Huang & Wang 2020) and 48 MSPs (Lorimer et al. 2015).

In the second step of the simulation, after generating a realisation of the Galactic pulsar population (for canonical pulsars or MSPs, respectively), we then simulate pulsar surveys using FAST and FASTA instrument parameters. The FAST survey parameters (including gain, system temperature, bandwidth, centre frequency, time and frequency resolution, etc.) are set according to FAST performance and survey description papers (e.g. Li et al. 2018; Jiang et al. 2019, 2020; Han et al. 2021). For FASTA survey, we apply the same survey parameter as FAST Galactic plane survey (Han et al. 2021). In the ideal coherent beam-forming process, an array consisting of  $N$  antennae would have a sensitivity  $N$  times better ( $G_{\text{array}} = N \times G_{\text{antenna}}$ ). In practice, we considered a phasing efficiency parameter of 0.94 (Chen et al. 2021) when estimating the gain value ( $G_{\text{array}} = 0.94 \times N \times G_{\text{antenna}}$ ). The gain value for FAST is 16 K/Jy, thus, the estimated gain for FASTA3 and FASTA6 are  $\sim 45$  K/Jy and  $\sim 90$  K/Jy, respectively.

For the cases of incoherent sum, the gain of an array consisting of  $N$  antennae would be  $G_{\text{array}} = \sqrt{N} \times G_{\text{antenna}}$ . Therefore, the incoherent gain for FASTA3 and FASTA6 are  $\sim 28$  K/Jy and  $\sim 40$  K/Jy.

We note that the sensitivity of FAST drops drastically when the zenith angle (ZA) is greater than  $26.4^\circ$ . According to Jiang et al. (2019), the gain of FAST is 16 K/Jy when  $ZA < 26.4^\circ$ , while it decreases as a linear function of ZA and becomes 11 K/Jy when  $ZA = 40^\circ$ . We have taken this effect into account in our simulation for both FAST and FASTA.

All the survey parameters we adopted for FAST and FASTA are summarised in Table 3. We use FASTA3 and FASTA6 to represent the coherent beam-forming cases. While for incoherent summing cases, we use FASTA3-i and FASTA6-i, respectively.

Table 3: System parameters used in the simulated survey with FAST and FASTA

	FAST	FASTA3-i	FASTA6-i	FASTA3	FASTA6
Survey degradation factor	0.8	0.8	0.8	0.8	0.8
Gain (K/Jy) <sup>†</sup>	16	28	40	45	90
Integration time (s)	300	300	300	300	300
Sampling time (ms)	0.2	0.2	0.2	0.2	0.2
System temperature (K)	20	20	20	20	20
Centre frequency (MHz)	1250	1250	1250	1250	1250
Bandwidth (MHz)	400	400	400	400	400
Channel bandwidth (MHz)	0.125	0.125	0.125	0.125	0.125
Number of polarizations	2	2	2	2	2
Full-width half maximum (arcmin)	3	3	3	3	3
Minimum RA (deg)	0	0	0	0	0
Maximum RA (deg)	360	360	360	360	360
Minimum DEC (deg)	-14	-14	-14	-14	-14
Maximum DEC (deg)	65	65	65	65	65
Minimum abs(Galactic latitude) (deg)	0	0	0	0	0
Maximum abs(Galactic latitude) (deg)	10	10	10	10	10
Fractional sky coverage (0-1)	1	1	1	1	1
Minimum signal-to-noise	9	9	9	9	9

<sup>†</sup> The values listed in this row are the gain value when pointing to  $ZA < 26.4^\circ$ . For  $26.4^\circ < ZA < 40^\circ$ , the gain value we applied is a linear function of ZA, which is  $G = G_{\text{zenith}} \times [1 - 0.0216(ZA - 26.4^\circ)]$ .

### 3 RESULT

#### 3.1 Detection prospects of Galactic CPs/MSPs with FASTA

With each set of the synthetic pulsar population model parameters summarised in Table 1 and Table 2, we simulate 20 realisations of pulsar populations. While for each realisation, we perform 20 times

survey simulations for each set of survey parameters listed in Table 3. Therefore, for each parameter combination, we run 400 times simulations in total to get the detection prospects for either canonical pulsars or MSPs. The results are summarised in Table 4 and Table 5.

For canonical pulsars that FAST is able to detect, the prediction numbers given by different models range from  $\sim 4200$  to  $8460$ , while for the most sensitive FASTA6 coherent beamform mode, the predicted detectable CPs range from  $\sim 8380$  to  $17330$ . These prediction numbers all include currently known pulsars. Therefore, when we consider the number of new CPs discoveries, we need to subtract  $\sim 1000$  known Galactic-plane CPs in the sky field of FAST/FASTA survey. For MSPs, FAST detection prospect given by different models range from  $\sim 520$  to  $1480$ , and the number of FASTA6 detectable MSPs range from  $\sim 1140$  to  $4680$ . Similar to the case of CPs, these prediction numbers include known MSPs, and when considering new MSPs discoveries,  $\sim 100$  known MSPs in the survey field need to be subtracted.

Figure 1 shows the Galactic distribution of the simulated pulsar population and predicted survey detection in polar coordinates. We choose the predicted result from the current FAST and the most sensitive FASTA6 coherent beamform mode to illustrate. The synthetic pulsar population of this example plot is generated based on snapshot mode with YK04 radial density distribution.

Table 4: Model parameters and the results for FAST and FASTA simulated survey on Galactic CPs.

Simulation mode	P-dist	L-dist	R-dist	Survey predicted detections ( $1\sigma$ ) <sup>†</sup>	
Snapshot	L06 lognormal	FK06 lognormal	L06	FAST	$6280 \pm 200$
				FASTA3-i	$8200 \pm 250$
				FASTA6-i	$9620 \pm 290$
				FASTA3	$10080 \pm 310$
				FASTA6	$12940 \pm 400$
			YK04	FAST	$8460 \pm 230$
				FASTA3-i	$11010 \pm 290$
				FASTA6-i	$12810 \pm 340$
				FASTA3	$13430 \pm 360$
				FASTA6	$17330 \pm 460$
Evolutionary	FK06 lognormal	$L = 0.18P^{-1.5}\dot{P}^{0.5}$ (B=12.65, FK06)	L06	FAST	$4200 \pm 140$
				FASTA3-i	$5400 \pm 170$
				FASTA6-i	$6230 \pm 200$
				FASTA3	$6520 \pm 210$
				FASTA6	$8380 \pm 270$
			YK04	FAST	$5080 \pm 180$
				FASTA3-i	$6520 \pm 240$
				FASTA6-i	$7560 \pm 280$
				FASTA3	$7910 \pm 290$
				FASTA6	$10160 \pm 370$
		Fan beam model (Huang & Wang 2020)	L06	FAST	$4460 \pm 170$
				FASTA3-i	$6010 \pm 240$
				FASTA6-i	$7230 \pm 280$
				FASTA3	$7670 \pm 290$
				FASTA6	$10640 \pm 390$
			YK04	FAST	$5650 \pm 220$
				FASTA3-i	$7600 \pm 270$
				FASTA6-i	$9070 \pm 320$
				FASTA6	$9590 \pm 340$
				FASTA6	$13290 \pm 470$

<sup>†</sup> The predicted detection number with  $1\sigma$  distribution dispersion.

### 3.2 Detection prospects of radio pulsars in M31 with FASTA

Up to now, astronomers haven't discovered radio pulsars in the nearby galaxy M31. FASTA will have great potential to make the breakthrough discovery in the detection of the first pulsar in M31. According to Savino et al. (2022), the distance of M31 is  $776 \pm 22$  kpc. Considering a time integration of 2 hours



Table 5: Model parameters and the results for FAST and FASTA simulated survey on Galactic MSPs.

Simulation mode	P-dist	L-dist	R-dist	Survey predicted detections ( $1\sigma$ ) <sup>†</sup>	
Snapshot	L15 lognormal	FK06 lognormal	L06	FAST	620±100
				FASTA3-i	800±130
				FASTA6-i	940±150
				FASTA3	990±160
				FASTA6	1300±200
			YK04	FAST	820±90
				FASTA3-i	1090±120
				FASTA6-i	1270±140
				FASTA6	1340±150
				FASTA6	1750±200
Evolutionary	L15 model as initial $P$ distribution	FK06 lognormal	L06	FAST	520±60
				FASTA3-i	700±80
				FASTA6-i	820±100
				FASTA3	860±100
				FASTA6	1140±140
			YK04	FAST	560±80
				FASTA3-i	740±110
				FASTA6-i	880±130
				FASTA6	930±140
				FASTA6	1240±190
			L06	FAST	1290±230
				FASTA3-i	1960±350
				FASTA6-i	2530±450
				FASTA6	2740±490
				FASTA6	4210±760
YK04	FAST	1480±190			
	FASTA3-i	2230±280			
	FASTA6-i	2830±360			
	FASTA6	3070±390			
	FASTA6	4680±610			

<sup>†</sup> The predicted detection number with  $1\sigma$  distribution dispersion.

for each pointing (corresponding to a total survey time of  $\sim 37$  hours with 10-min overhead, covering M31 in 17 pointings), and a bandwidth of 400 MHz, dual-polarisation observation, FAST will be able to detect pulsars with L-band luminosity greater than 670 mJy kpc<sup>2</sup> at the distance of M31. While for FASTA3-i, FASTA6-i, FAST3, and FASTA6, the corresponding luminosity limit at L-band would be 380 mJy kpc<sup>2</sup>, 270 mJy kpc<sup>2</sup>, 240 mJy kpc<sup>2</sup>, and 120 mJy kpc<sup>2</sup>, respectively. We can then estimate the detection prospect of radio pulsars in M31 based on how many pulsars in M31 have luminosity above the detection limit of each configuration. We assume the M31 has a similar pulsar population to our Galaxy.

We considered three types of population models: 1) the snapshot model with FK06 lognormal luminosity distribution; 2) the evolutionary model with FK06 luminosity distribution; 3) the evolutionary model with fanbeam luminosity distribution. These models are the same as what we used in the previous sections when we estimated the detection prospect of Galactic canonical pulsars, but we did not distinguish the L06 and YK04 radial distribution for M31 pulsar detection prospect estimation.

For the snapshot model with FK06 lognormal luminosity distribution, the corresponding pulsar detection numbers of FAST, FASTA3-i, FASTA6-i, FAST3, FASTA6 are 1, 3, 7, 9, 28, respectively. For the evolutionary model with FK06 luminosity distribution, the corresponding pulsar detection numbers are 12, 29, 47, 60, 164, respectively. For the evolutionary model with fanbeam luminosity distribution, the corresponding pulsar detection numbers are 34, 55, 77, 92, 188, respectively.

Although the detection prospect predicted by those three models are quite different, they all show the same trend as the instrument sensitivity increases, especially in the case of FASTA6. Thus, there is a good chance to detect a significant amount of radio pulsars in M31.

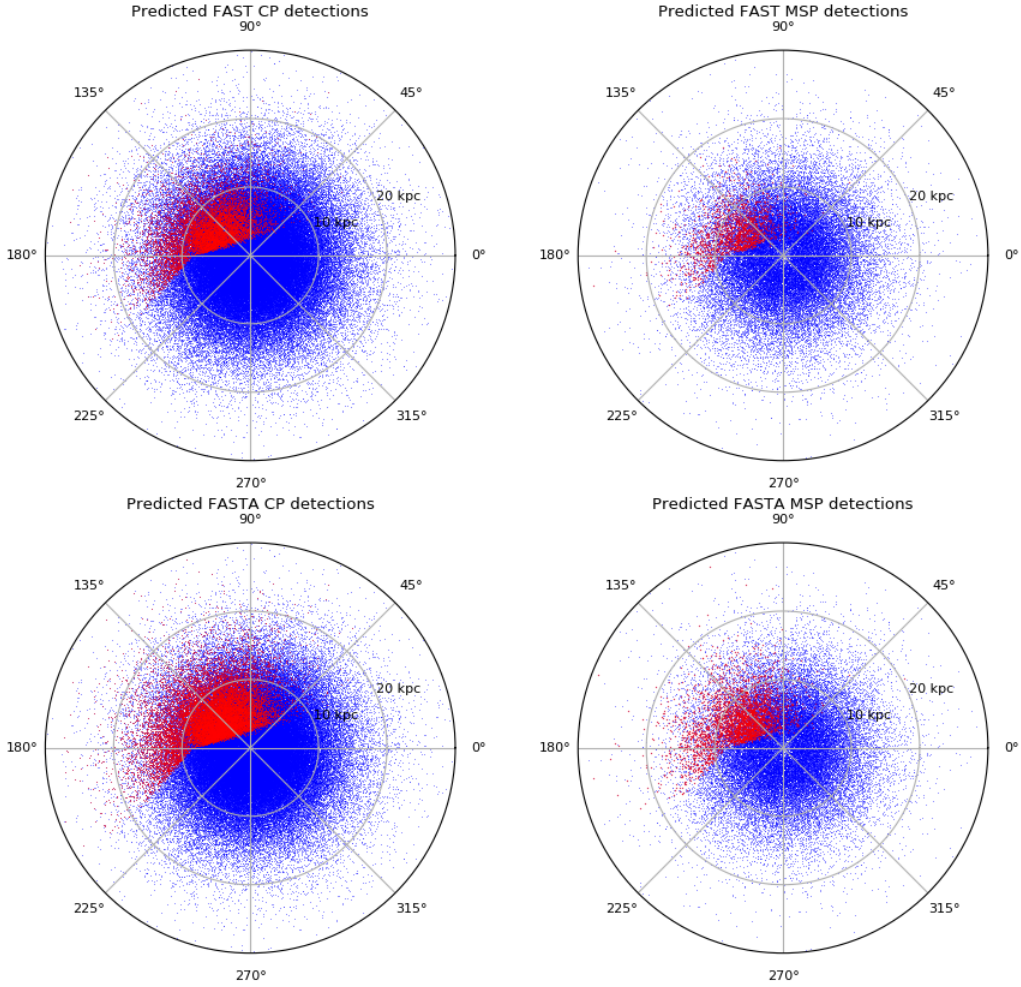


Fig. 1: Galactic distribution of the simulated pulsar population (blue dots) and predicted FAST/FASTA6 survey detection (red dots) in polar coordinates (top-view from the Galactic North pole). The synthetic pulsar population of this example plot is generated based on snapshot mode with YK04 radial density distribution.

### 3.3 Survey time estimation

The total observable sky for FAST with galactic latitude  $|b| < 10^\circ$  is  $4035 \text{ deg}^2$ . If FASTA makes use of the Phased Array Feed (PAF) with FWHM of  $30'$ , then the survey will need 20550 pointings in total. As the planned integration time is 5 minutes, the entire survey will need to take 1713 observing hours.

If we include 10 minutes overhead for each pointing, the survey will take 5138 hours in total. Since the overhead will take a significant amount of time for each pointing, it's natural for us to raise a question — what if we increase the observing integration time for each pointing, will it improve the return-cost-rate of the survey in terms of the pulsar detection number vs. total survey time? To explore the answers, we run simulations by setting the observing integration time to 10, 15, 20 minutes along with different combinations of pulsar population model and survey configuration (i.e. different gain) listed in Section 3.1. According to the radiometer equation, the telescope sensitivity is proportional to

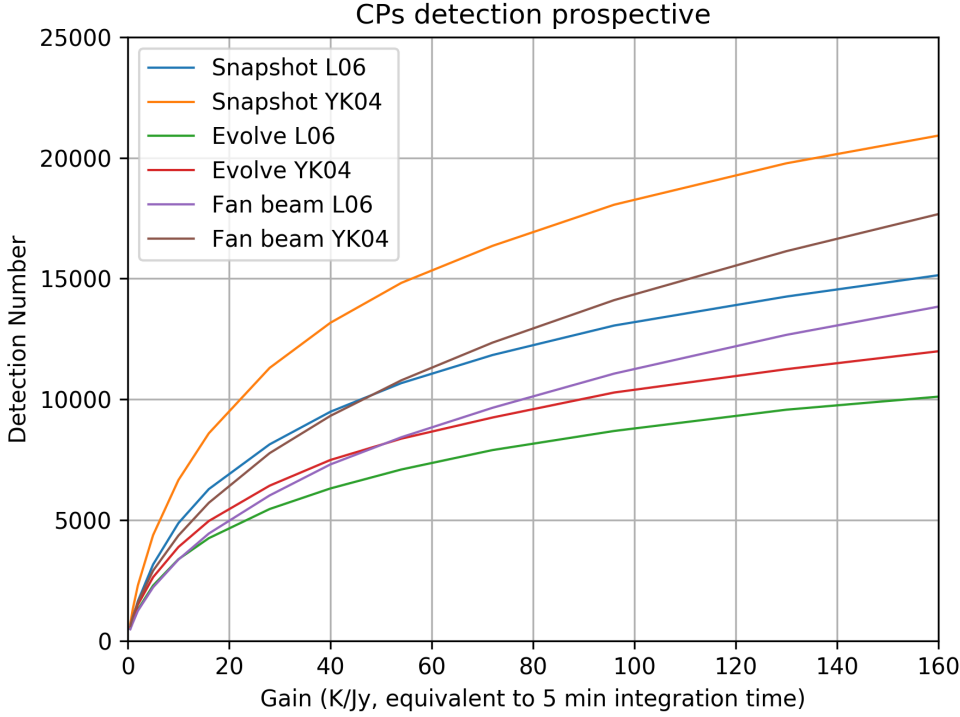


Fig. 2: Number of canonical pulsars detected in simulated surveys with 5-min integration time for different gain values, remaining parameters we used in these simulations are all from Table 3. For other integration times that we want to compare (e.g. 10, 15, 20 min as listed in the top panel of Table 6), we can calculate the corresponding gain value that equivalent to 5-min integration time,  $G_{\text{equiv}} = G \times \sqrt{t_{\text{int}}/5\text{min}}$ . Different color lines indicate different pulsar population models.

the instrument gain and the square-root of the integration time. In order to make it more concise, we convert different integration time to a gain-increment equivalent to 5-min integration time,  $G_{\text{equiv}} = G \times \sqrt{t_{\text{int}}/5\text{min}}$ . The corresponding equivalent gain values are listed in the top panel of Table 6. We then simulate CPs detection numbers as a function of different gain values (ranging from 0.5 to 160) for different population models, with 5-min integration time. The result can be found in Figure 2.

Using the snapshot model with L06 radial distribution (blue line in Figure 2) as an example, we list the simulated pulsar detection numbers with different observing integration time and different survey configurations in the middle panel of Table 6. We also convert those numbers to percentages relative to FAST 5-min integration result (the bottom panel of Table 6), so that we can get a more straightforward idea of the detection number increment. Comparing the survey time increment percentage and detection number increment percentage, we find that 5-min integration time is still the most efficient survey setting.

#### 4 DISCUSSION AND CONCLUSION

In this work, we estimated pulsar detection prospects for simulated FAST and FASTA pulsar surveys with galactic latitude  $|b| < 10^\circ$ , using various pulsar population models. We tested models from both the snapshot and evolutionary types, with different combinations of distribution parameters. Our results indicate that FASTA could detect around ten thousand canonical pulsars and well-over thousands of

Table 6: Simulated pulsar detection numbers using the snapshot model with L06 radial distribution.

	Total survey time (hours)	Gain (equivalent to 5-min integration time)				
		FAST	FAST3-i	FAST6-i	FAST3	FAST6
5 min	5138	16	28	40	45	90
10 min	6850	23	40	57	64	127
15 min	8563	28	48	69	78	156
20 min	10275	32	56	80	90	180
	Total survey time (hours)	Detection numbers				
		FAST	FAST3-i	FAST6-i	FAST3	FAST6
5 min	5138	6287	8160	9479	9943	12758
10 min	6850	7420	9437	10855	11336	14169
15 min	8563	8129	10240	11688	12146	15026
20 min	10275	8654	10806	12278	12755	15623
	Total survey time (hours)	Detection numbers (% relative to FAST 5 min)				
		FAST	FAST3-i	FAST6-i	FAST3	FAST6
5 min	100%	100%	130%	151%	158%	203%
10 min	133%	118%	150%	173%	180%	225%
15 min	167%	129%	163%	186%	193%	239%
20 min	200%	138%	172%	195%	203%	248%

millisecond pulsars. Additionally, we estimated the yield of searching for pulsars in the nearby spiral galaxy M31 using FASTA, and found that it has a potential to discover around a hundred new radio pulsars. Furthermore, we also found that the most efficient observational settings in terms of the observing time and discovery number for a Galactic-plane pulsar survey is to apply 5-min integration time with a PAF.

We estimated the pulsar detection prospect of using both the incoherent sum or coherent beam-forming data analysis method for FASTA data. The baseline design of FASTA has not been determined yet, but as a first-order approximation, we can consider the maximum baseline of FASTA to be  $\sim 300$  km. Since the baseline is 1000 times longer than the effective diameter of FAST (300 m), we need to form  $10^6$  coherent beams to cover the area of one current FAST beam. Therefore, to cover the sky area of the proposed survey, the number of beams we need to form is on the order of  $10^{12}$ . This will inevitably result in a significant increase in data processing demand, which seems to be infeasible with current computational instruments and techniques. Nevertheless, we can remain hopeful that the requirement can be met in a few decades since Moore’s Law suggests that the computational capability would increase one order of magnitude in 5 to 7 years, and there might be other potential technique revolution in the coming future. While for the beginning, a pulsar survey with incoherently summing data would be more realistic, and we can first apply coherent beam-forming data for some specific sky areas such as M31 or selected globular clusters.

With the high sensitivity of FASTA, it is likely that more pulsars (especially long-period pulsars, intermittent pulsars and RRATs) could be detected when adopting additional single pulse search. According to existing pulsar surveys with large spherical radio telescopes, [Deneva et al. \(2009\)](#) found that the single pulse search led to 13% extra pulsar discoveries from Arecibo PALFA survey, [Han et al. \(2021\)](#) found a 14% extra yield from FAST GPPS survey, while as a drift scan survey with each point source drifts across the 3’ beam in 12 s, the CRAFTS survey of FAST benefits more from single pulse search and has discovered  $\sim 31\%$  additional pulsars using this method. These findings indicate that there may be an extra 10-20% of detectable pulsars which are not accounted for in our analysis.

Our limited understanding of the low end of pulsar radio luminosity function leads to a large range for the predicted pulsar yields. The current parameters are mostly derived from Parkes Multibeam survey pulsar sample (e.g. [Yusifov & Küçük 2004](#); [Lorimer et al. 2006](#); [Faucher-Giguère & Kaspi 2006](#); [Lorimer et al. 2015](#)), and to build pulsar population model, it is a standard practice to calibrate the distribution parameter with PMPS sample (e.g. [Rajwade et al. 2017](#); [Huang & Wang 2020](#)). So there is no surprise that the pulsar detection numbers predicted by different models and distribution parameters can converge nicely on PMPS surveys, but result in very different outcomes when applying different observing settings like FAST or FASTA which have significantly higher gain. Therefore, the result of

how many new weak pulsars can be discovered in FAST and FASTA survey will provide us a very useful constraint of pulsar luminosity distribution.

Han et al. (2021) suggested the FAST pulsar surveys will probably finish with fewer new pulsar discoveries than the predicted number, indicating that the current model extrapolated from PMPS might overestimate the undetected Galactic pulsar population. This also means that the known pulsars discovered in PMPS survey constitute a larger proportion of the overall pulsar population than we previously expected. If that is the case, some possible explanations include: (a) there are fewer pulsars at the low end of the luminosity function than we thought; (b) the distances of the pulsars estimated using their DM and the Galactic electron density model are uncertain; (c) scattering smear from the interstellar medium makes it difficult for us to detect far-away pulsars.

In conclusion, our estimation of the pulsar detection prospect of FASTA based on a variety of models generally converges to a consistent picture. Due to our limited knowledge of the real Galactic pulsar population, it is hard to pinpoint the exact number of pulsar detections of the FASTA pulsar survey with a narrow range of uncertainty. We look forward to the outcome of currently ongoing FAST pulsar surveys and future FASTA pulsar surveys with good completeness, as they will provide significantly better constraints on the Galactic pulsar population and its distribution parameters.

**Acknowledgements** This work is supported by the National Natural Science Foundation of China (NSFC) grant No. 12203070 and the National SKA Program of China No. 2020SKA0120200. This work is also supported by the NSFC grant No. 12041303, 11873067, the CAS-MPG LEGACY project. Mengyao Xue is supported by the Cultivation Project for FAST Scientific Payoff and Research Achievement of CAMS-CAS and Project funded by China Postdoctoral Science Foundation No. 2021M703237. Hongguang Wang is supported by NSFC 12133004, the National SKA Program of China No. 2020SKA0120101, the Science and Technology Program of Guangzhou (No. 202102010466) and the Astronomy Science and Technology Research Laboratory of Department of Education of Guangdong Province, China. This research made use of `PsRPopPy`<sup>3</sup>, `PsRPopPy2`<sup>4</sup>, and `astropy`<sup>5</sup>.

## References

- Astropy Collaboration, Robitaille, T. P., Tollerud, E. J., et al. 2013, *A&A*, 558, A33 [13](#)
- Astropy Collaboration, Price-Whelan, A. M., Sipőcz, B. M., et al. 2018, *AJ*, 156, 123 [13](#)
- Backer, D. C., Kulkarni, S. R., Heiles, C., Davis, M. M., & Goss, W. M. 1982, *Nature*, 300, 615 [1](#)
- Bates, S. D., Lorimer, D. R., Rane, A., & Swiggum, J. 2014, *MNRAS*, 439, 2893 [3](#), [13](#)
- Bates, S. D., Lorimer, D. R., & Verbiest, J. P. W. 2013, *MNRAS*, 431, 1352 [2](#)
- Caleb, M., Heywood, I., Rajwade, K., et al. 2022, *Nature Astronomy*, 6, 828 [1](#)
- Cameron, A. D., Li, D., Hobbs, G., et al. 2020, *MNRAS*, 495, 3515 [2](#)
- Carlberg, R. G., & Innanen, K. A. 1987, *AJ*, 94, 666 [5](#)
- Chen, W., Barr, E., Karuppusamy, R., Kramer, M., & Stappers, B. 2021, *Journal of Astronomical Instrumentation*, 10, 2150013 [7](#)
- Contopoulos, I., & Spitkovsky, A. 2006, *ApJ*, 643, 1139 [3](#), [4](#)
- Cordes, J. M., Freire, P. C. C., Lorimer, D. R., et al. 2006, *ApJ*, 637, 446 [2](#)
- Deneva, J. S., Cordes, J. M., McLaughlin, M. A., et al. 2009, *ApJ*, 703, 2259 [12](#)
- Eatough, R. P., Kramer, M., Lyne, A. G., & Keith, M. J. 2013, *MNRAS*, 431, 292 [2](#)
- Edwards, R. T., Bailes, M., van Straten, W., & Britton, M. C. 2001, *MNRAS*, 326, 358 [7](#)
- Emmering, R. T., & Chevalier, R. A. 1989, *ApJ*, 345, 931 [3](#)
- Faucher-Giguère, C.-A., & Kaspi, V. M. 2006, *ApJ*, 643, 332 [2](#), [3](#), [4](#), [12](#)
- Faulkner, A. J., Stairs, I. H., Kramer, M., et al. 2004, *MNRAS*, 355, 147 [2](#)
- Gould, D. M. 1994, *Structure and polarization of pulsar radio emission beams*, PhD thesis, University of Manchester, UK [3](#)

<sup>3</sup> <https://github.com/samb8s/PsRPopPy> (Bates et al. 2014)

<sup>4</sup> <https://github.com/devanshkv/PsRPopPy2>

<sup>5</sup> <https://www.astropy.org> (Astropy Collaboration et al. 2013, 2018)

- Han, J. L., Wang, C., Wang, P. F., et al. 2021, arXiv e-prints, arXiv:2105.08460 2, 7, 12, 13
- Hobbs, G., Faulkner, A., Stairs, I. H., et al. 2004, MNRAS, 352, 1439 2
- Huang, W. J., & Wang, H. G. 2020, ApJ, 905, 144 3, 4, 5, 7, 8, 12
- Jacoby, B. A., Bailes, M., Ord, S. M., Knight, H. S., & Hotan, A. W. 2007, ApJ, 656, 408 7
- Jiang, P., Yue, Y., Gan, H., et al. 2019, Science China Physics, Mechanics, and Astronomy, 62, 959502 7
- Jiang, P., Tang, N.-Y., Hou, L.-G., et al. 2020, Research in Astronomy and Astrophysics, 20, 064 7
- Knispel, B., Eatough, R. P., Kim, H., et al. 2013, ApJ, 774, 93 2
- Kramer, M., Xilouris, K. M., Lorimer, D. R., et al. 1998, ApJ, 501, 270 4
- Kramer, M., Bell, J. F., Manchester, R. N., et al. 2003, MNRAS, 342, 1299 2
- Kuijken, K., & Gilmore, G. 1989, MNRAS, 239, 651 5
- Li, D., Wang, P., Qian, L., et al. 2018, IEEE Microwave Magazine, 19, 112 2, 7
- Lorimer, D. R., Faulkner, A. J., Lyne, A. G., et al. 2006, MNRAS, 372, 777 2, 3, 4, 12
- Lorimer, D. R., Esposito, P., Manchester, R. N., et al. 2015, MNRAS, 450, 2185 4, 7, 12
- Lyne, A. G., Manchester, R. N., & Taylor, J. H. 1985, MNRAS, 213, 613 4
- Lyne, A. G., Ritchings, R. T., & Smith, F. G. 1975, MNRAS, 171, 579 4
- Manchester, R. N., Hobbs, G. B., Teoh, A., & Hobbs, M. 2005, AJ, 129, 1993 1
- Manchester, R. N., Lyne, A. G., Camilo, F., et al. 2001, MNRAS, 328, 17 2, 3
- McEwen, A. E., Spiewak, R., Swiggum, J. K., et al. 2020, ApJ, 892, 76 2
- Mdzinarishvili, T. G., & Melikidze, G. I. 2004, A&A, 425, 1009 4
- Morris, D. J., Hobbs, G., Lyne, A. G., et al. 2002, MNRAS, 335, 275 2
- Nan, R. 2006, Science in China: Physics, Mechanics and Astronomy, 49, 129 2
- Nan, R., Peng, B., Qiu, Y. H., et al. 2002, SKA Memo, 8481, 17 2
- Nan, R., Li, D., Jin, C., et al. 2011, International Journal of Modern Physics D, 20, 989 2
- Peng, B., & Nan, R. 1998, Symposium - International Astronomical Union, 179, 93–94 2
- Qian, L., Yao, R., Sun, J., et al. 2020, The Innovation, 1, 100053 2
- Rajwade, K. M., Lorimer, D. R., & Anderson, L. D. 2017, MNRAS, 471, 730 3, 4, 5, 6, 9, 12
- Ridley, J. P., & Lorimer, D. R. 2010, MNRAS, 404, 1081 3
- Savino, A., Weisz, D. R., Skillman, E. D., et al. 2022, ApJ, 938, 101 8
- Smits, R., Lorimer, D. R., Kramer, M., et al. 2009, A&A, 505, 919 4
- Stovall, K., Lynch, R. S., Ransom, S. M., et al. 2014, ApJ, 791, 67 2
- Swiggum, J. K., Lorimer, D. R., McLaughlin, M. A., et al. 2014, ApJ, 787, 137 2
- Tan, C. M., Bassa, C. G., Cooper, S., et al. 2018, ApJ, 866, 54 1
- Tauris, T. M., & Manchester, R. N. 1998, MNRAS, 298, 625 5
- Vivekanand, M., & Narayan, R. 1981, Journal of Astrophysics and Astronomy, 2, 315 4
- Wang, H. G., Pi, F. P., Zheng, X. P., et al. 2014, ApJ, 789, 73 4
- Yusifov, I., & Küçük, I. 2004, A&A, 422, 545 4, 12